MATIMYÁS MATEMATIKA
ISSN 0115-6926

Journal of the Mathematical Society of the Philippines
Vol. 45 No. 2 (2022) pp. 49-64

Classifying Relative Equilibria and Relative Periodic Solutions in Two Mutually Delay-Coupled Stuart-Landau Oscillators

Andrei A. Domogo
Department of Mathematics and Computer Science
University of the Philippines Baguio
UP Drive, Baguio City, Philippines
aadomogo1@up.edu.ph

Juancho A. Collera
Department of Mathematics and Computer Science
University of the Philippines Baguio
UP Drive, Baguio City, Philippines
jacolllera@up.edu.ph

Abstract

A model of two oscillators represented by a system of mutually delay-coupled Stuart-Landau equations that are fully symmetric is examined. In this study, we focused on symmetric solutions of the system. Particularly, we used a group-theoretic approach to obtain the relative equilibria and the relative periodic solutions. By varying the coupling phase, numerical continuation is performed to generate the two branches of symmetric relative equilibria. For a branch of symmetric relative equilibria, symmetry-preserving and symmetry-breaking steady-state and Hopf bifurcations are identified. These classification of bifurcations followed from the isotypic decomposition of the physical space corresponding to the system of oscillators. Emanating branch of relative equilibria and relative periodic solutions with broken symmetry from symmetry-breaking steady-state and Hopf bifurcations, respectively, are generated. Moreover, branch of relative periodic solutions emanating from Hopf bifurcations had preserved or broken symmetry depending on the classification of the Hopf bifurcation. These findings emphasized how the symmetry approach organized the way of looking for solutions to the two-oscillator system. Solutions with full symmetry are first obtained then solutions with lesser symmetry are then found through symmetry-breaking bifurcations. Finally, branches of fold and Hopf bifurcations are generated by performing two-parameter continuation.

Keywords: Stuart-Landau Oscillators, Equivariant Dynamical System, Symmetry-Breaking Bifurcations, Numerical Continuation
2020 MSC: 37C81, 34K04, 34K24, 65P30

1 Introduction

Oscillations can be pictured as a recurring pattern. These are very common in the natural world and in artificial creations. Examples seen in nature are the beating of the heart,

menstrual cycles, firing of neurons, glowing of fireflies, and the chirping of crickets. With the objective of investigating and analyzing oscillating behavior, researchers developed models of oscillators such as the Lorenz system [1], Lang-Kobayashi equations [2], Lotka-Volterra equations [3], and Stuart-Landau equations [4], among others. These models put forward a way to study repetitive and collective behavior, which contribute to different fields of science and engineering [5].

One main motivation for the study of oscillator systems is their ability to coordinate their movement or synchronize as a result of interaction. Comprehension of the mechanisms underlying in the synchronization of oscillator systems found in nature resulted in the study of collective behavior of coupled oscillators [6]. It was observed that coupled oscillators are able to synchronize under different types and strength of coupling [7, 8, 9]. Theoretically, the study of solutions to oscillator systems that possess a certain kind of synchrony presents a systematic way of finding other solutions through symmetry breaking. In this study, we considered a symmetric system of two mutually delay-coupled Stuart-Landau oscillators with the aim of classifying the symmetry of its solutions. We used a group theoretic approach to show that the symmetry of the solutions follow from the symmetry of the system of equations representing the coupled oscillators. Also, we perform numerical continuation and bifurcation analysis to generate branches of solutions with different symmetries.

2 Symmetric Two-Oscillator System

In this section, we present the model of two mutually delay-coupled Stuart-Landau (SL) oscillators that are completely symmetric [10] and examine the properties of both the model and its solutions. Particularly, we are going to describe the symmetry of the model and characterize its symmetric solutions.

The model is represented by the system of SL equations given by

$$\begin{cases} \dot{a}_1 &= a_1(1-|a_1|^2) + i\beta a_1|a_1|^2 + ke^{iC_p}a_2(t-\tau) \\ \dot{a}_2 &= a_2(1-|a_2|^2) + i\beta a_2|a_2|^2 + ke^{iC_p}a_1(t-\tau), \end{cases} \tag{1}$$

where β is the coupling between amplitude and phase, k is the coupling strength, C_p is the coupling phase, and τ is the delay in coupling.

2.1 Symmetry Group and its Isotropy Subgroups

We claim that system (1) has symmetry group isomorphic to $\mathbb{Z}_2 \times S^1$. To show this, we note that a homomorphism $\rho : \mathbb{Z}_2 = \langle\gamma\rangle \to GL(2,\mathbb{C})$ defined by $e \mapsto \mathbb{I}_2, \quad \gamma \mapsto \begin{bmatrix} 0 & 1 \\ 1 & 0 \end{bmatrix}$, is a representation of $\mathbb{Z}_2$ on $\mathbb{C}^2$. The action of γ on $[a_1, a_2]^\top \in \mathbb{C}^2$ is then given by $\gamma \cdot [a_1, a_2]^\top = [a_2, a_1]^\top$. Moreover, the homomorphism $\phi : S^1 \to GL(2,\mathbb{C})$ defined by $e^{i\theta} \mapsto e^{i\theta}\mathbb{I}_2$ is a representation of S^1 on $\mathbb{C}^2$. The action of $e^{i\theta}$ on $[a_1, a_2]^\top \in \mathbb{C}^2$ is then given by $e^{i\theta} \cdot [a_1, a_2]^\top = [e^{i\theta}a_1, e^{i\theta}a_2]^\top$. Now, if we define $f : \mathbb{C}^2 \to \mathbb{C}^2$ by $f([a_1, a_2]^\top) = [\dot{a}_1, \dot{a}_2]^\top$, then $f(\gamma \cdot [a_1, a_2]^\top) = \gamma \cdot [\dot{a}_1, \dot{a}_2]^\top$ and $f(e^{i\theta} \cdot [a_1, a_2]^\top) = e^{i\theta} \cdot [\dot{a}_1, \dot{a}_2]^\top$. Therefore, system (1) has symmetry group isomorphic to $\mathbb{Z}_2 \times S^1$.

The isotropy subgroups of $\mathbb{Z}_n \times S^1$ are twisted subgroups [11]. In particular, the maximal nontrivial isotropy subgroups of $\mathbb{Z}_2 \times S^1$ are isomorphic to $\mathbb{Z}_2$. They are $\mathbb{Z}_2(\gamma) := \langle\gamma, e^{i2\pi}\rangle$ and $\mathbb{Z}_2(\gamma, \pi) := \langle\gamma, e^{i\pi}\rangle$ [12]. Figure 1 presents the lattice diagram of the maximal isotropy subgroups of $\mathbb{Z}_2 \times S^1$.

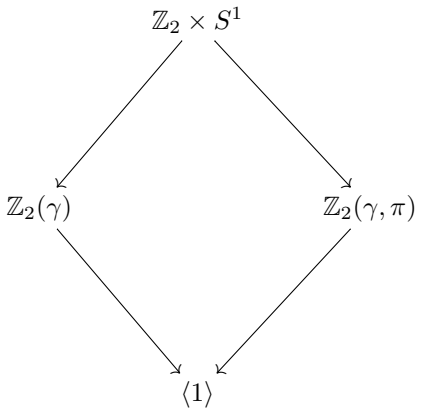

Figure 1: Isotropy subgroup lattice diagram of $\mathbb{Z}_2 \times S^1$.

2.2 Symmetric Relative Equilibria

The S^1-symmetry of system (1) brings about *relative equilibria* (RE) of the form

$$\begin{array}{rcl} a_1(t) & = & r_1 e^{i\omega t + i\sigma_1} \\ a_2(t) & = & r_2 e^{i\omega t + i\sigma_2}, \end{array} \tag{2}$$

which are solutions with period $2\pi/\omega$ [13]. Here, $r_1, r_2 \geq 0$ are the amplitudes, ω is the frequency, and σ_1, σ_2 are phase shifts. These are also called *rotating/continuous waves*. Such form of basic solutions that were considered in Lang-Kobayashi system of oscillators are called *compound laser modes* [12, 14].

Our goal is to find the symmetric RE of the form given in (2). These are the rotating waves that are fixed by a particular isotropy subgroup. Note that the fixed-point subspace of $\mathbb{Z}_2(\gamma)$ is $Fix(\mathbb{Z}_2(\gamma)) = \{[a, a]^\top \in \mathbb{C}^2 | a = re^{i\omega t + i\sigma}\}$ and the fixed-point subspace of $\mathbb{Z}_2(\gamma, \pi)$ is $Fix(\mathbb{Z}_2(\gamma, \pi)) = \{[a, -a]^\top \in \mathbb{C}^2 | a = re^{i\omega t + i\sigma}\}$. We call the elements of $Fix(\mathbb{Z}_2(\gamma))$ as the *in-phase RE* and the elements of $Fix(\mathbb{Z}_2(\gamma))$ as the *anti-phase RE*.

To find in-phase RE, we substitute ansatz $a_1 = a_2 = re^{i\omega t + i\sigma}$ to system (1). We get, $i\omega = 1 - r^2 + i\beta r^2 + k\cos(C_p - \omega\tau) + ik\sin(C_p - \omega\tau)$. The real and imaginary parts, $r^2 = 1 + k\cos(C_p - \omega\tau)$ and $\omega = \beta r^2 + k\sin(C_p - \omega\tau)$, respectively, are combined to get $\omega = \beta + k(\beta\cos(C_p - \omega\tau)) + \sin(C_p - \omega\tau))$. Using the identity,

$$\alpha\cos\vartheta + \sin\vartheta = \sqrt{1+\alpha^2}\sin(\vartheta + \arctan(\alpha)) \quad \text{for} \quad \alpha \geq 0,$$

we have that

$$\omega = \beta + k\sqrt{1+\beta^2}\sin(C_p - \omega\tau + \arctan(\beta)). \tag{3}$$

Similarly, to get anti-phase RE, we substitute ansatz $a_1 = re^{i\omega t + i\sigma}$ and $a_2 = -a_1$ to system (1). We get,

$$\omega = \beta - k\sqrt{1+\beta^2}\sin(C_p - \omega\tau + \arctan(\beta)). \tag{4}$$

Note that ω given by equations (3) and (4) always exists since its value(s) is(are) the intersection(s) of a diagonal line passing at the origin and a sine wave. When the value of ω is known in equations (3) and (4), then the value of r can be computed. In particular,

$r = \sqrt{1 + k\cos(C_p - \omega\tau)}$ and $r = \sqrt{1 - k\cos(C_p - \omega\tau)}$ for the in-phase and anti-phase RE, respectively. The values for ω and r will then correspond to a RE. In summary, we have the following theorem whose proof is given by the derivations above.

Theorem 2.1. *The RE of system (1) with $\mathbb{Z}_2(\gamma)$ and $\mathbb{Z}_2(\gamma, \pi)$ symmetry can be obtained by solving for ω in equations (3) and (4), respectively. In particular, in-phase RE are given by*

$$a_1 = a_2 = re^{i\omega t + i\sigma}$$

where $r = \sqrt{1 + k\cos(C_p - \omega\tau)}$ and anti-phase RE are given by

$$a_1 = re^{i\omega t + i\sigma} \quad \textit{and} \quad a_2 = re^{i\omega t + i\sigma + i\pi} = -a_1$$

where $r = \sqrt{1 - k\cos(C_p - \omega\tau)}$.

Note that these formulas for ω for the in-phase and anti-phase solutions are already presented in [10]. In this study, we demonstrated how these formulas follow from our classification of solutions of the system through a group-theoretic approach.

2.3 Branches of Symmetric Relative Equilibria

We utilize Theorem 2.1 to calculate the symmetric RE for system (1). Here, we use the following parameter values: $\beta = 4$, $k = 0.7$, $C_p = 0$, and $\tau = 3$. We perform the computations in Matlab by modifying a program developed by Erzgraber et al. for a two-laser system [14]. Once a symmetric RE is found using Theorem 2.1, we then perform numerical continuation using DDE-Biftool [15, 16] by varying C_p. We choose C_p as the continuation parameter because system (1) has 2π-translational symmetry in C_p. The 2π-translational symmetry permits us to observe a whole branch, looking at its stability and bifurcation points, for C_p varied on an interval of length 2π. Figure 2 presents the branch of in-phase RE in the (ω, r)-plane while Figure 3 presents in-phase and anti-phase RE in the (C_p, r)-plane

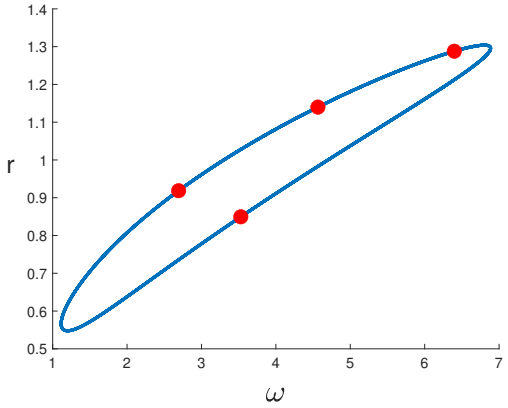

Figure 2: Branch of in-phase RE in the (ω, r)-plane. The four dots with (ω, r) values approximately given by $(2.6930, 0.9186)$, $(3.5289, 0.8495)$, $(4.5650, 1.1399)$, and $(6.3982, 1.2879)$, correspond to the in-phase RE calculated using Theorem 2.1. The branch of in-phase and anti-phase RE overlap in this plane.

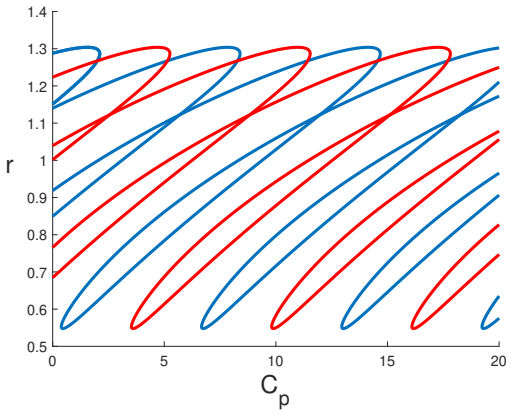

Figure 3: Branch of in-phase (blue curve) and anti-phase (red curve) RE in the (C_p, r)-plane. The curves are half a period (π) out of phase. The anti-phase branch is basically the same as the in-phase branch except for the π translation.

3 Classification of Codimension-One Bifurcations

The codimension-one bifurcations of system (1) can be obtained numerically using DDE-Biftool. However, further classification of these bifurcations into symmetry-breaking or

symmetry-preserving is possible through a group-theoretic approach. We will discuss this approach in this section.

Note that DDE-Biftool is able to analyze the stability of RE and can identify steady-state and Hopf bifurcation points as shown in Figure 4. However, there is no classification of bifurcations obtained from this numerical result.

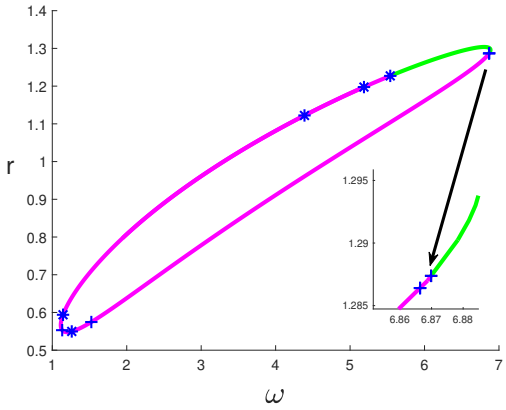

Figure 4: Stability plot for the branch of in-phase RE in the (ω, r)-plane obtained using DDE-Biftool. The stable part is colored green while the unstable part is colored magenta. Moreover, steady-state $(+)$ and Hopf bifurcation points $(*)$ are identified.

In the following discussion, we provide a classification of these bifurcation points into symmetry-breaking or symmetry preserving. This can be done by looking at the isotypic decomposition of the physical space corresponding to the system of Stuart-Landau equations. Previous studies involving coupled symmetric systems have used this group-theoretic approach [11, 12, 17, 18].

Theorem 3.1. *Let V_1 and V_2 be subspaces of $\mathbb{R}^4$ with basis elements $v_1 = v \cdot [1,1]^\top$ and $v_2 = v \cdot [-1,1]^\top$, respectively, where $v \in \mathbb{R}^2$, then $\mathbb{Z}_2(\gamma)$ lies in the isotropy subgroup of solutions (of system (1) near an in-phase RE) coming from V_1.*

Proof. We first linearize system (1) around an in-phase RE. Note that a general solution of system (1) can be written in the form $a_i(t) = r_i(t)e^{i\phi_i(t)}$, $i = 1, 2$. Using this notation, system (1) in polar form is given by

$$\begin{aligned}\dot{r}_i(t) &= r_i(t)(1 - r_i^2(t)) + kr_{i+1}(t-\tau)\cos(C_p + \phi_{i+1}(t-\tau) - \phi_i(t))\\ \dot{\phi}_i(t) &= \beta r_i^2(t) + k\tfrac{r_{i+1}(t-\tau)}{r_i(t)}\sin(C_p + \phi_{i+1}(t-\tau) - \phi_i(t)),\end{aligned}$$

which can be written in the form $\dot{X}(t) = F(X(t), Y(t))$ where $X(t) = [r_1(t), \phi_1(t), r_2(t), \phi_2(t)]$ and $Y(t) = X(t-\tau)$. To get the linear variational equation around an in-phase RE, we compute $M_1 := \frac{\partial F}{\partial X}$ and $M_2 := \frac{\partial F}{\partial Y}$ where both matrices are evaluated at an in-phase RE.

We get $M_1 = \begin{bmatrix} \bar{A} & 0 \\ 0 & \bar{A} \end{bmatrix}$, where $\bar{A} = \begin{bmatrix} 1-3r^2 & kr\sin(C_p-\omega\tau) \\ 2\beta r - \frac{k}{r}\sin(C_p-\omega\tau) & -k\cos(C_p-\omega\tau) \end{bmatrix}$ and $M_2 = \begin{bmatrix} 0 & \bar{B} \\ \bar{B} & 0 \end{bmatrix}$, where $\bar{B} = \begin{bmatrix} k\cos(C_p-\omega\tau) & -kr\sin(C_p-\omega\tau) \\ \frac{k}{r}\sin(C_p-\omega\tau) & k\cos(C_p-\omega\tau) \end{bmatrix}$. The linear variational equation around an in-phase RE is then given by $\dot{X}(t) = M_1X(t) + M_2X(t-\tau)$ and the corresponding characteristic equation is $\det\Delta(\lambda) = 0$ where $\Delta(\lambda) = \lambda I - M_1 - e^{-\lambda\tau}M_2$. If we let $A := \lambda I - \bar{A}$ and $B := -e^{-\lambda\tau}\bar{B}$, then $L := \Delta(\lambda) = \begin{bmatrix} A & B \\ B & A \end{bmatrix}$.

Now, our objective is to block diagonalize L. This simplifies the computation of eigenvalues by dealing with smaller matrices. Moreover, it provides the needed classification of the codimension-one bifurcations. We begin by noting that $\mathbb{Z}_2(\gamma)$ acts irreducibly on the subspaces V_1 and V_2 with basis elements $v_1 = v\cdot[1,1]^\top$ and $v_2 = v\cdot[-1,1]^\top$, respectively, where $v \in \mathbb{R}^2$. Observe that $L(v_1) = \begin{bmatrix} A & B \\ B & A \end{bmatrix}\begin{bmatrix} v \\ v \end{bmatrix} = \begin{bmatrix} (A+B)v \\ (A+B)v \end{bmatrix}$ and $L(v_2) = \begin{bmatrix} A & B \\ B & A \end{bmatrix}\begin{bmatrix} -v \\ v \end{bmatrix} = \begin{bmatrix} (A-B)(-v) \\ (A-B)v \end{bmatrix}$ Hence, we obtain the block-diagonalized form $\begin{bmatrix} A+B & 0 \\ 0 & A-B \end{bmatrix}$.

Note that the action of $\mathbb{Z}_2(\gamma)$ decomposes the physical space $\mathbb{R}^4$ into $V_1\oplus V_2$. As observed in the block diagonalization process, the block $A+B$ corresponds to the action of L on V_1 and the block $A-B$ corresponds to the action of L on V_2. If the critical eigenvalue γ comes form $A+B$, we get bifurcations with symmetry $\mathbb{Z}_2(\gamma)$ because $\mathbb{Z}_2(\gamma)$ acts trivially on V_1. To say it in another way, $\mathbb{Z}_2(\gamma)$ lies in the isotropy subgroup of solutions coming from V_1. Moreover, since the symmetry is preserved, we expect saddle-node bifurcations [12, 17]. If the critical eigenvalue γ comes from the block $A-B$, we get symmetry breaking bifurcations because $\mathbb{Z}_2(\gamma)$ does not act trivially on V_2. Moreover, since the action of $\mathbb{Z}_2(\gamma)$ on V_2 is of order 2 and symmetry is broken, we expect pitchfork bifurcations [12, 17, 19].

□

3.1 Steady-State Bifurcations

To find steady-state bifurcations along the branch of in-phase RE we look for the values of C_p at the intersection of the transcendental equation (3) corresponding to an in-phase RE and $\det\Delta(\lambda)|_{\lambda=0} = 0$. Note that $\det\Delta(\lambda)|_{\lambda=0} = 0$ is equivalent to $|A+B|_{\lambda=0} = 0$ or $|A-B|_{\lambda=0} = 0$. We have that $|A+B|_{\lambda=0}$ and $|A-B|_{\lambda=0}$ are given by

$$\begin{aligned} |A+B|_{\lambda=0} &= (1+k\tau\cos(C_p-\omega\tau))(-1+3r^2-k\cos(C_p-\omega\tau)) \\ &- 2\beta r^2 k\tau\sin(C_p-\omega\tau) \end{aligned}$$

and

$$\begin{aligned} |A-B|_{\lambda=0} &= 2k\{[\cos(C_p-\omega\tau)][-1+3r^2]+k \\ &- 2\beta r^2\sin(C_p-\omega\tau)+k\sin^2(C_p-\omega\tau)\}. \end{aligned}$$

The intersections of equation (3) with $|A+B|_{\lambda=0}=0$ and $|A-B|_{\lambda=0}=0$ are shown in Figure 5.

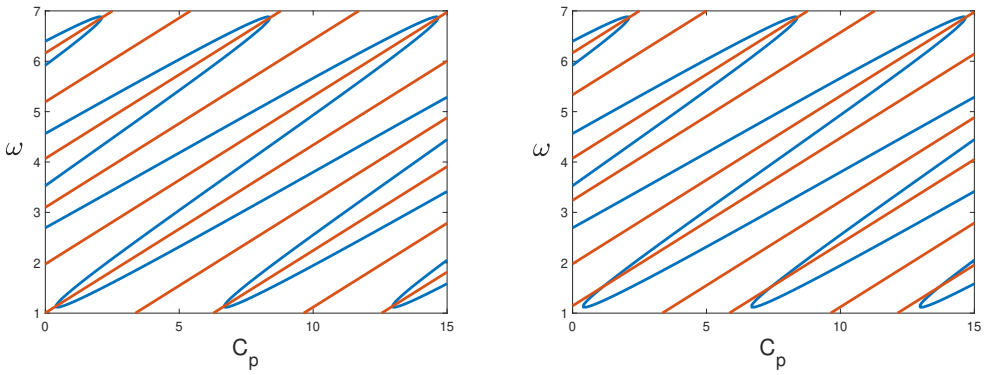

Figure 5: (Left Panel): Intersection of the branch of in-phase RE (blue curve) with the orange curve corresponding to $|A+B|_{\lambda=0}=0$, which occurs at $\omega\approx 1.1331$ and 6.8668. (Right Panel): Intersection of the branch of in-phase RE (blue curve) with the orange curve corresponding to $|A-B|_{\lambda=0}=0$, which occurs at $\omega\approx 1.5253$ and 6.8706.

3.2 Hopf Bifurcations

To find Hopf bifurcations along the branch of in-phase RE, we look for C_p values satisfying the transcendental equation (3) corresponding to an in-phase RE and $\det\Delta(\lambda)|_{\lambda=i\alpha}=0$. Note that $\det\Delta(\lambda)|_{\lambda=i\alpha}=0$ is equivalent to $|A+B|_{\lambda=i\alpha}=0$ or $|A-B|_{\lambda=i\alpha}=0$. First, we solve for C_p in equation (3). The distinct C_p values modulo 2π are given by the following.

$$C_p = \arcsin\left(\frac{\omega-\beta}{k\sqrt{1+\beta^2}}\right)+\omega\tau-\arctan(\beta) \tag{5}$$

$$C_p = \pi-\arcsin\left(\frac{\omega-\beta}{k\sqrt{1+\beta^2}}\right)+\omega\tau-\arctan(\beta) \tag{6}$$

We substitute C_p given in equations (5) and (6) to the equations $|A+B|_{\lambda=i\alpha}=0$ and $|A-B|_{\lambda=i\alpha}=0$ to get equations in $\mathbb{C}$ that are dependent on α and ω. For the resulting equations, the intersection of the real part and imaginary part equated to zero will give us the ω values where Hopf bifurcations occur. These intersections are shown in Figure 6 and 7.

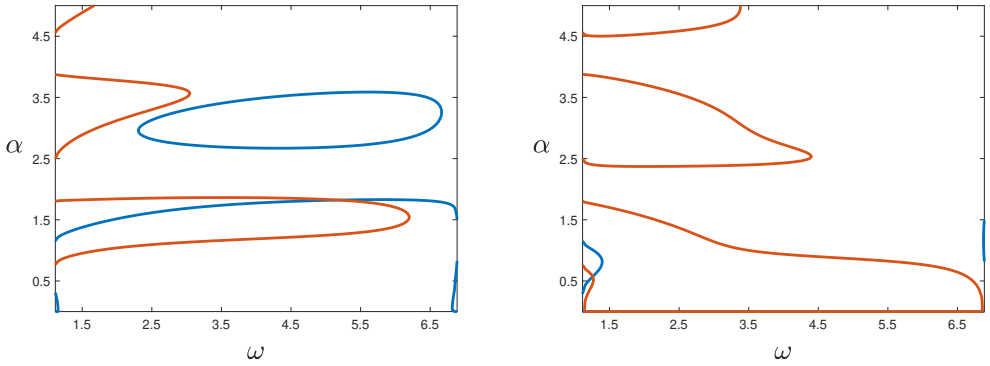

Figure 6: Intersection of the real part (blue curve) and imaginary part (red curve) of $|A + B|_{\lambda=i\alpha} = 0$ for C_p given by equation (5) (left panel) and (6) (right panel). In total, we get two intersections corresponding to symmetry-preserving Hopf bifurcations, which occurs at $\omega \approx 5.1850$ (left panel) and 1.2599 (right panel).

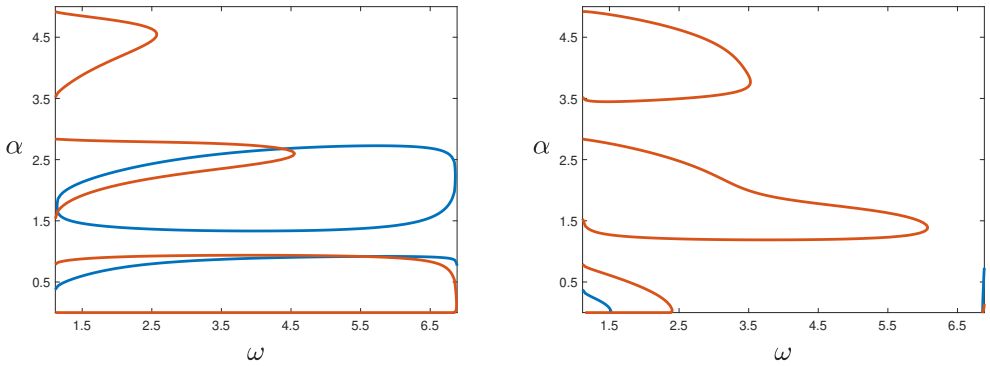

Figure 7: Intersection of the real part (blue curve) and imaginary part (red curve) of $|A - B|_{\lambda=i\alpha} = 0$ for C_p given by equation (5) (left panel) and (6) (right panel). In total, we get three intersections corresponding to symmetry-breaking Hopf bifurcations, which occurs at $\omega \approx 1.1443$, 4.3851, and 5.5399 (left panel) and none in the right panel.

Overall, we were able to find 4 steady-state and 5 Hopf bifurcations along the branch of in-phase RE. Classification of these bifurcations into symmetry-preserving or symmetry-breaking is shown in Figure 8. Using a similar process, classification of steady-state and Hopf bifurcation points along the branch of anti-phase RE can be located and classified. In the (ω, r)-plane we get the same figure as in Figure 8. In the (C_p, r)-plane we get the same figure except for a translation of π.

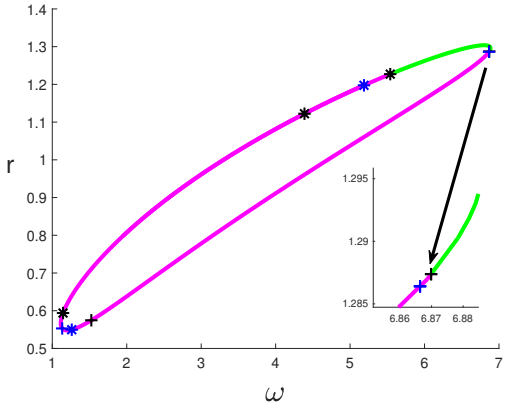

Figure 8: Classification of steady-state (+) and Hopf (∗) bifurcation points along the branch of in-phase RE. Symmertry-preserving bifurcations are colored blue and symmetry-breaking bifurcations are colored black.

3.3 Branches of Relative Equilibria and Relative Periodic Solutions

We now obtain the branches of RE and relative periodic solutions from the classified bifurcations in the previous section. Particularly, we generate the emanating branch of RE from the pitchfork bifurcations, and the branches of relative periodic solutions emanating from Hopf bifurcations. From section 3, we expect pitchfork bifurcations from the symmetry-breaking steady-state bifurcation points. We use this knowledge to generate an emanating branch of RE with no symmetry. This is performed in DDE-Biftool and this new branch of RE is presented in Figure 9. Moreover, relative periodic solutions emanating from Hopf bifurcation are also generated in DDE-Biftool. Figure 10 presents these branches of relative periodic solutions where their symmetry is preserved or broken depending on the classification of the Hopf bifurcation.

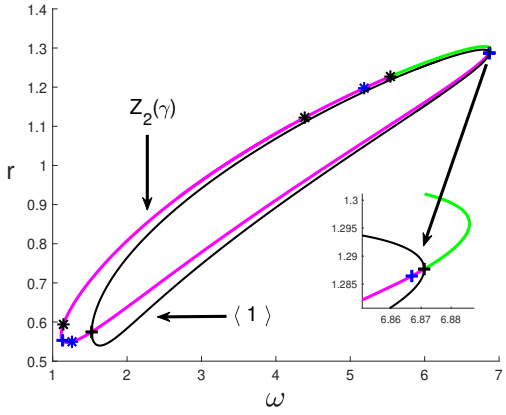

Figure 9: Bifurcating branch of RE with no symmetry (black curve) emanating from pitchfork bifurcations.

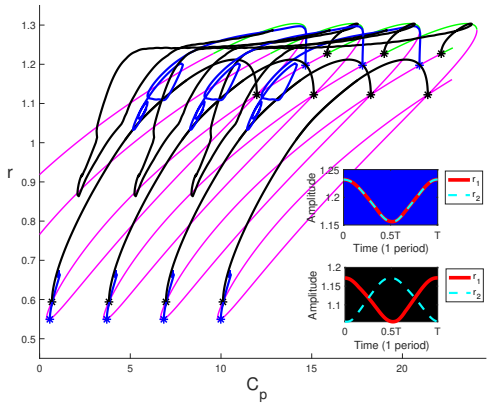

Figure 10: Bifurcating branches of relative periodic solutions emanating from Hopf bifurcations. Relative periodic solutions emanating from symmetry-preserving bifurcations have equal amplitude while those emanating from symmetry-breaking bifurcations have amplitude which are half a period translated.

3.4 Two-parameter Continuation

Lastly, branches of steady-state fold and Hopf bifurcations can be obtained numerically by performing two-parameter continuation in DDE-Biftool. We vary the parameters k and C_p and plot on the (C_p, r)-plane the generated branch of steady-state fold bifurcations of RE (Figure 11) and branches of Hopf bifurcations of RE (Figure 12). In Figure 13, branches

of fold and Hopf bifurcations points are plotted in the two-parameter space to show the changes in numbers of these bifurcations depending on the values of the parameters.

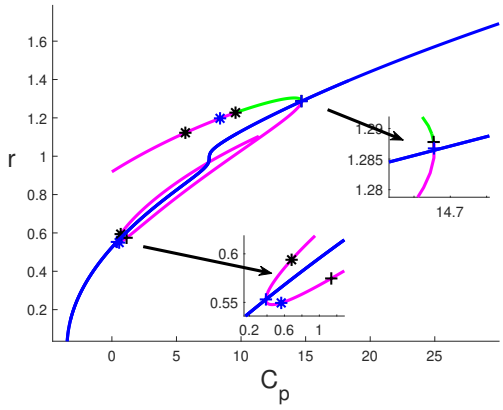

Figure 11: Continuation of fold bifurcations (blue curve) of RE generated by varying k and C_p.

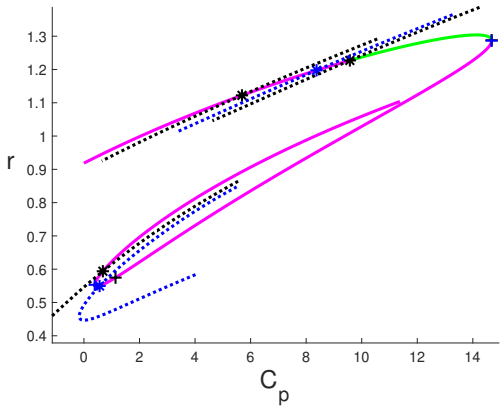

Figure 12: Continuation of Hopf bifurcations (dotted curves) of RE generated by varying k and C_p.

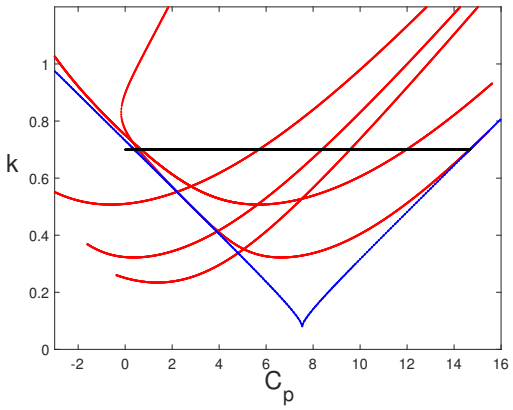

Figure 13: Branches of fold (blue) and Hopf (red) bifurcation points generated by varying k and C_p. The points in the black line are the k and C_p values corresponding to the branch of RE where we have performed classification of codimension-one bifurcations.

4 Summary

In summary, we have obtained RE and relative periodic solutions to the system of two oscillators described by Stuart-Landau equations by considering the isotropy subgroups of symmetry group of the system. This led to obtaining the RE that are in-phase and anti-phase. Numerical continuation in DDE-Biftool generated branches of RE that are in-phase and anti-phase. Along the branch of in-phase RE, steady-state and Hopf bifurcations are determined and then classified into symmetry-preserving or symmetry-breaking. Here, the characteristic matrix of the linear variational equation around an in-phase RE was block diagonlized using the isotypic decomposition of the physical space corresponding to the system of oscillators. The classification of the bifurcations into symmetry-preserving or symmetry-breaking follows from these block diagonalization. In DDE-Biftool, emanating branch of RE with no symmetry are generated from symmetry-breaking steady-state bifurcations, i.e. pitchfork bifurcations, and emanating branch of relative periodic solutions are generated from Hopf bifurcations. Moreover, emanating branch of relative periodic solution showed that the oscillators have equal amplitude if they arise from symmetry-preserving Hopf bifurcations and have amplitude that are half a period translated if they arise from symmetry-breaking Hopf bifurcations. Lastly, branches of fold and Hopf bifurcations are generated by varying the coupling strength and coupling phase.

5 Acknowledgement

The authors would like to thank Professor Priscilla Supnet-Macansantos, PhD, for introducing us to the field of dynamical systems and inspiring us to advance mathematics research and teaching in Northern Luzon.

References

[1] E. Lorenz. Deterministic nonperiodic flow. *Journal of the Atmospheric Sciences*, 20:130–141, 1963.

[2] R. Lang and K. Kobayashi. External optical feedback effects on semiconductor injection laser properties. *IEEE Journal of Quantum Electron*, 16:347–355, 1980.

[3] A. Lotka. Contribution to the theory of periodic reaction. *The Journal of Physical Chemistry*, 14:271–274, 1910.

[4] J. Stuart. On the non-linear mechanics of wave disturbances in stable and unstable parallel flows part 1. the basic behaviour in plane poiseuilee flow. *Journal of Fluid Mechanics*, 9(3):353–370, 1960.

[5] E. Panteley, A. Loria, and A. El-Ati. On the stability and robustness of stuart-landau oscillators. *International Federation of Automatic Control*, pages 645–650, 2015.

[6] E. Panteley, A. Loria, and A. El-Ati. Practical dynamic consensus of stuart-landau oscillators over heterogeneous networks. *International Journal of Control*, 2018.

[7] S. Krishnagopal, J. Lehnert, W. Poel, A. Zakharova, and E. Schöll. Synchronization patterns: from network motifs to hierarchical networks. *Philosophical Transactions Royal Society A*, 375:20160216, 2017.

[8] A. Domogo and J. Collera. Symmetric solutions to a system of mutually delay-coupled oscillators with conjugate coupling. *Journal of Physcis: Conference Series*, 1123(012028), 2018.

[9] S. Tajima, H. Singh, S. Nakabayashi, T. Singla, and P. Parmananda. The emergence of synchrony behavior in weakly coupled electrochemical oscillators via a 'metallic plate'. *Journal of Electroanalytical Chemistry*, 769:16–20, 2016.

[10] O. D'Huys, R. Vicente, J. Danckaert, and I. Fischer. Synchronization and symmetry breaking of delay-coupled oscillators: on the role of phase and amplitude instabilities. *Proc. of SPIE*, 7720, 2010.

[11] P. Buono and J. Collera. Symmetry-breaking bifurcations in rings of delay-coupled semiconductor lasers. *SIAM Journal on Applied Dynamical Systems*, 14:1868–1898, 2015.

[12] J. Collera. Symmetry-breaking bifurcations in two mutually delay-coupled lasers. *International Journal of Philippine Science and Technology*, 8:17–21, 2015.

[13] S. Yanchuk and J. Sieber. Relative equilibria and relative periodic solutions in systems with time-delay and s^1 symmetry. *arXiv: Mathematical Physics*, 2013.

[14] H. Erzgraber, B. Krauskopf, and D. Lenstra. Compound laser modes of mutually delay-coupled lasers. *SIAM Journal on Applied Dynamical Systems*, 5:30–65, 2006.

[15] K. Engelborghs, T. Luzyanina, and D. Roose. Numerical bifurcation analysis of dela differential equations using dde-biftool. *ACM Trans. Math. Softw.*, 28(1):1–21, 2002.

[16] J. Sieber, K. Engelborghs, T. Luzyanina, G. Samaey, and D. Roose. *DDE-BIFTOOL v.3.1.1 Manual - Bifurcation analysis of delay differential equations*, 2017.

[17] A. Domogo and J. Collera. Classification of codimension-one bifurcations in a tetrad of lasers with feed forward coupling. *AIP Conference Proceedings*, 1787, 2016.

[18] M. Golubitsky, I. Stewart, and D. Schaeffer. *Singularities and Groups in Bifurcation Theory*, volume II. Springer-Verlag, 1988.

[19] P. Chossat and R. Lauterbach. *Methods in Equivariant Bifurcations and Dynamical Systems*. World Scientific Publishing Co. Pte. Ltd., 2000.

This page is intentionally left blank